

Measurement of Skin Permeation/Penetration of Nanoparticles for Their Safety Evaluation

Eriko Kimura,^a Yuichiro Kawano,^a Hiroaki Todo,^a Yoshiaki Ikarashi,^b and Kenji Sugibayashi^{*a,c}

^aFaculty of Pharmaceutical Sciences, Josai University; ^cLife Science Research Center, Josai University; 1–1 Keyakidai, Sakado, Saitama 350–0295, Japan; ^bNational Institute of Health Sciences; 1–18–1 Kamiyoga, Setagaya-ku, Tokyo 158–8501, Japan. Received February 2, 2012; accepted June 5, 2012

The aim of the present study was to quantitatively evaluate the skin permeation/penetration of nanomaterials and to consider their penetration pathway through skin. Firstly, penetration/permeation of a model fluorescent nanoparticle, Fluoresbrite[®], was determined through intact rat skin and several damaged skins. Fluoresbrite[®] permeated through only needle-punctured skin. The permeation profiles of soluble high molecular compounds, fluorescein isothiocyanate-dextran (FITC-dextran, FDs), with different molecular weights were also measured for comparison. The effects of molecular sizes and different skin pretreatments on the skin barrier were determined on the skin penetration/permeation of Fluoresbrite[®] and FDs. Fluoresbrite[®] was not permeated the intact skin, but FDs were permeated the skin. The skin distribution of titanium dioxide and zinc oxide nanoparticles was also observed after topical application of commercial cosmetics. Nanoparticles in sunscreen cosmetics were easily distributed into the groove and hair follicles after their topical application, but seldom migrated from the groove or follicles to viable epidermis and dermis. The obtained results suggested that nanoparticles did not permeate intact skin, but permeated pore-created skin. No or little permeation was observed for these nanomaterials through the stratum corneum.

Key words nanoparticle; titanium dioxide; skin permeation; skin penetration; damaged skin

Recently, nanotechnology has been a focus as a useful technology producing new nanometer-sized materials with new functions and properties.¹⁾ Many nanomaterials have been developed using this technology, and various commercial products, such as medicines, foods, cosmetics and chemicals, are available on a global basis. Nanomaterials have been defined as nanometer-sized chemicals or nanometer-scaled aggregates with a one-dimensional length of 1–100 nm.²⁾ There are two kinds of nanomaterials: non-intentional and intentional nanomaterials. The former is exemplified by ash rising from volcanos and mountain fires as well as nanoparticles exhausted from diesel fumes, and the latter is industrial nanomaterials produced with several aims. Exposure of humans to non-intentional nanomaterials may be reduced by the progress of science and technology regarding human safety. Since many nanomaterials have been produced very rapidly, particular care should be taken regarding intensive or industrial nanomaterials, which are divided into biodegradable and non-biodegradable.³⁾ Liposomes, niosomes and nanosized emulsions are biodegradable nanomaterials. Toxicity may be a concern for monomers and metabolites of nanomaterials. Fullerenes and titanium dioxide (TiO₂) nanoparticles are examples of non-biodegradable nanomaterials. The toxicity and bioaccumulation of these compounds should be evaluated to confirm their safety.

Possible exposure sites of nanomaterial are the trachea, gastrointestinal tracts and skin. Cosmetics are commercial products that contain many nanomaterials, and many sunscreen cosmetics and foundations sometimes contain titanium dioxide (TiO₂) and zinc oxide (ZnO) nanoparticles. Since these cosmetics are applied daily to the skin surface, the skin penetration and safety of these nanomaterials are a concern. Wu *et al.* reported that titanium dioxide nanoparticles were migrated into other organs after permeated through the skin

by continuous apply.⁴⁾ It is urgent to determine the skin penetration/permeation rate and to clarify the penetration/permeation pathway of the materials. Many reports have already suggested that these nanoparticles do not permeate the skin.^{5,6)} However, it is very difficult to quantitatively measure the skin permeation rate of titanium dioxide and zinc oxide nanoparticles through intact and healthy human and animal skin.⁷⁾ In addition, few reports have shown a quantitative penetration/permeation of titanium dioxide and zinc oxide nanoparticles through skin.

In the present study, Fluoresbrite[®] (fluorescent polystyrene latex spheres, particle size: 50 nm) was used as an easily detectable and non-dissolved model nanoparticle, and *in vitro* permeation experiments of the spheres were carried out through intact and wounded rat skin with different pretreatments. The permeation profiles of soluble high molecular compounds, fluorescein isothiocyanate-dextran (FITC-dextran, FDs) with different molecular weights through skin were also measured for comparison. The effects of different molecular sizes and pretreatments on the skin barrier were determined for the skin penetration/permeation of Fluoresbrite[®] and FDs. In addition, the skin surface distribution of titanium dioxide and zinc oxide nanoparticles was observed after topical application of commercial cosmetics.

THEORETICAL

Type of Material-Permeable Membranes Material-permeable membranes can be classed into three groups.⁸⁾ Type I is a dissolution-diffusion membrane in which materials dissolve and permeate through the membrane. A silicone membrane is an example of Type I membrane that is sometimes used as an alternative to human or animal stratum corneum. Type II is a porous membrane through which materials smaller than the pore size can permeate, for example, a dialysis membrane. Type III is a composite of dissolution-diffusion

The authors declare no conflict of interest.

* To whom correspondence should be addressed. e-mail: sugib@josai.ac.jp

and porous membranes.

Permeation through skin mainly occurs by the dissolution-diffusion phenomenon; that is, materials must dissolve in the membrane so that they can permeate the skin; however, it was reported recently that hair follicles must be an important skin permeation pathway for hydrophilic and macromolecular compounds.⁹⁾ Hair follicles are assumed to have a porous route as a Type II membrane. High molecular weight compounds and nanomaterials that are not dissolved in the skin may permeate through the hair follicular pathway.

Skin Permeability Coefficient and Desquamation Rate

The permeability coefficient (P , cm/s) is a quantitative index of the skin penetration and permeation of materials. The stratum corneum generally consists of about 20 corneocyte layers with a thickness of about 20 μm . If a 1 μm corneocyte layer is desquamated from the outermost stratum corneum per day, the desquamation ratio (P_{des}) is 1.0 $\mu\text{m}/\text{d}$, that is, about 10^{-9} cm/s. If the permeability coefficient of a certain material is less than the P_{des} , material that moved through the first corneocyte layer over 24 h is not further transferred to the second layer due to desquamation of the first layer.¹⁰⁾ Thus, material with P less than P_{des} is not theoretically transferred to the lower layer of the stratum corneum when the dominant permeation route is through the stratum corneum. Three categories can be established by the relationship between the magnitude of P and P_{des} as follows: (i) when $P - P_{\text{des}} \gg 0$, material permeates the skin, (ii) when $P \approx P_{\text{des}}$, material penetrates the skin, and (iii) when $P - P_{\text{des}} \ll 0$, material does not permeate or penetrate the skin.

Generally, materials diffuse through and permeate the skin according to their concentration gradient though the skin barrier (stratum corneum). The skin permeation rate (dQ/dt) of material per unit area is expressed by the following Eq. (1), Fick's 1st law of diffusion in the steady state.

$$\frac{dQ}{dt} = \frac{D \cdot K \cdot C_d}{L} \quad (1)$$

In addition, the permeability coefficient (P) is expressed as follows:

$$P = \frac{D \cdot K}{L} \quad (2)$$

where D is the diffusion coefficient in the skin barrier, K is the partition coefficient between the skin barrier and vehicle, C_d is the concentration of the applied compound and L is the barrier thickness of the skin.

MATERIALS AND METHODS

Materials Fluoresbrite® yellow green plain microspheres (50 nm in average diameter) were purchased from Polyscience, Inc. (Warrington, PA, U.S.A.). FDs (FD-4, FD-20, FD-40, FD-70, FD-250, FD-2000) were purchased from Sigma Aldrich Co. (St. Louis, MO, U.S.A.). Table 1 summarizes the physicochemical properties of FDs. Sunscreen (Allie Comfortable Protector EX) was purchased from Kanebo Cosmetic Inc. (Tokyo, Japan). All other reagents and solvents were of reagent grade and used without further purification.

Animals Male hairless rats (WBN/ILA-Ht, ca. 200–250 g) were supplied by Life Science Research Center, Josai University (Sakado, Saitama, Japan). Porcine ear skins (LWD strain) were from Saitama Experimental Animal Laboratory (Sugito,

Saitama, Japan). All animal experiments were approved by the Institutional Animal Care and Use Committee of Josai University.

In Vitro Skin Permeation Experiment The skin permeation of Fluoresbrite® and FDs was assessed using excised hairless rat abdominal skin. After the rats had been anesthetized by intraperitoneal injection of sodium pentobarbital (50 mg/kg), the left and right abdominal skin was excised. The skin samples have ca. 0.6–0.7 mm. Stripped hairless rat skin was also used after removing the stratum corneum from the abdominal area by stripping 20 times with adhesive tape (Cellophane tape; Nichiban Co., Ltd., Tokyo, Japan). Needle-punctured skin was treated one time with a 20–30 G needle (20 G; regular-beveled, 23–27 G; short-beveled, and 30 G; used in dentistry; all from Terumo Co., Tokyo, Japan) to puncture skin to 10 mm depth from the skin surface in the effective permeation area (One pore was created in the effective permeation area). In the preparation of needle-punctured skin, the abdominal skin was excised and set on the diffusion cell using Aron Alpha® (Toagosei Co., Ltd., Tokyo, Japan). We confirmed that the needle had completely penetrated the skin. Razor-treated skin with two wounds at 5 mm distance and 0.5 mm depth was made using a razor (Feather double-edged razor S; Feather Safety Razor Co., Ltd., Osaka, Japan) on the stratum corneum side. The depth (0.5 mm) was selected to reach the wound at top dermis and not to penetrate the cut through the excised skin. In the preparation of razor-treated skin, a razor was sandwiched between wooden chopsticks and pulled at constant pressure to make two parallel wounds at a distance of 0.5 mm in the effective permeation area. Razor-treated skin was prepared under anesthesia. Fat on the dermis side was carefully trimmed off with scissors.

These skin membranes were mounted on a side-by-side diffusion cell (effective diffusion area: 0.95 cm²). Phosphate-buffered saline (PBS, pH 7.4) (3.0 mL) was applied to the epidermal and dermal sides and left for one hour to remove autogenic fluorescence from skin and to hydrate the stratum corneum. Skin resistance was then measured using an impedance meter (Advance, Tokyo, Japan) with Ag and AgCl electrodes at 10 Hz for the alternating current supply. After PBS had been removed from the epidermal and dermal sides, 0.26% Fluoresbrite® suspension in PBS or FDs solution in PBS (1.0 mg/mL FD-4, 1.0 mg/mL FD-20, 7.5 mg/mL FD-40, 7.5 mg/mL FD-70, and 10 mg/mL FD-250, 10 mg/mL FD-2000 on the intact skin: 1.0 mg/mL FDs on the stripped skin, razor-treated skin and needle-punctured skin) was applied to the epidermal side and 3.0 mL fresh PBS was again applied to the dermal side. The receiver solution (0.50 mL) was sampled 0 h from the dermal side compartment, and the same volume of

Table 1. Physicochemical Properties of FITC-Dextrans (FDs)

FDs	M.W. (kDa)	Stokes diameter, d (nm)	Log d (nm in d)
FD-4	3.38–4.40	2.8 ⁽¹⁾	0.45
FD-20	21.2	6.6 ⁽¹⁾	0.82
FD-40	35.6–38.5	9.0 ⁽¹⁾	0.95
FD-70	69.8	12.0 ⁽¹⁾	1.08
FD-250	250	21.0 ⁽²⁾	1.32
FD-2000	2000	41.6 ⁽³⁾	1.62

Refer to the references for the number in brackets.

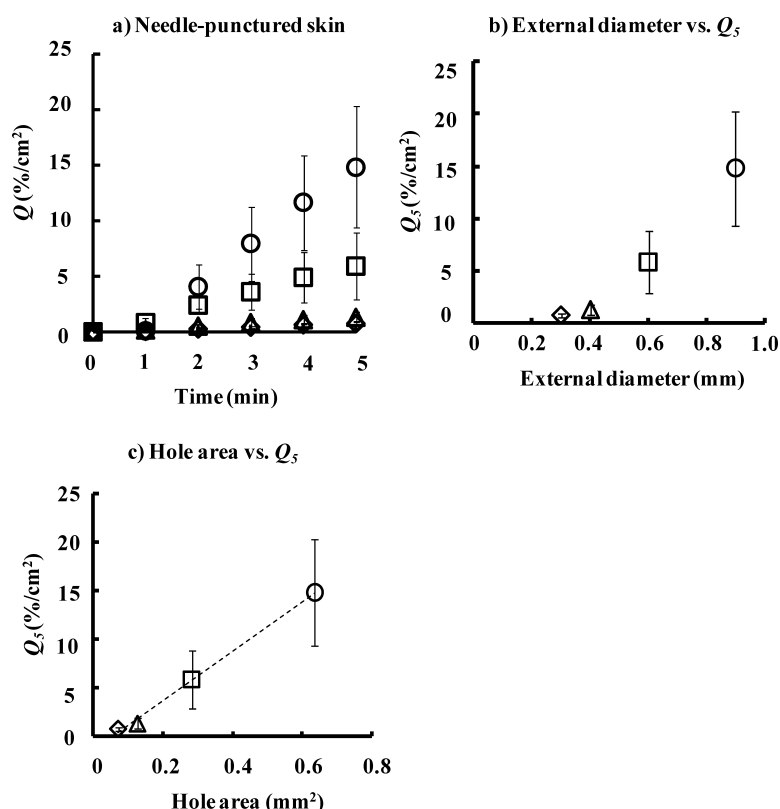


Fig. 1. Effect of Needle-Puncture on the Skin Permeation of Fluoresbrite®

a: Time course of changes in the cumulative fraction of Fluoresbrite® that permeated through needle-punctured hairless rat skin, b: relationship between external diameter and the cumulative amount of Fluoresbrite® that permeated needle-punctured skin over 5 min (Q_5), and c: relationship between pore area by needle-puncture and the cumulative amount of Fluoresbrite® that permeated through needle-punctured skin over 5 min (Q_5). Symbols: ○: 20G needle (external diameter: 0.9 mm), □: 23G needle (0.6 mm), △: 27G needle (0.4 mm), ◇: 30G needle (0.3 mm). Each point represents the mean \pm S.E. ($n=3-4$).

fresh PBS was added to continue the permeation experiments. Polysorbate 80/PBS solution (0.1%) was used to prevent air from entering the pore in the needle-punctured skin. It was confirmed that the permeation rate was not changed through other damaged skins using polysorbate 80/PBS solution. The experiment was performed at 32°C, and the epidermal and dermal sides were stirred by magnetic stirrers. Aliquots (0.50 mL) were periodically withdrawn from the dermal side compartment, and the same volume of fresh PBS was added to keep the volume constant. Fluoresbrite® or FDs concentration in each sample was determined by a fluorescence spectrophotometer (RF5300; Shimadzu, Kyoto, Japan) at excitation and emission wavelengths of 441 and 486 nm (Fluoresbrite®) or 490 nm and 520 nm (FDs).

Morphological Evaluation of Skin The skin surface of hairless rats was carefully rinsed with PBS several times to remove Fluoresbrite® attached to the skin after the permeation experiments. The skin specimens were embedded in Super Cryoembedding Medium (Leica Microsystems, Wetzlar, Germany) and frozen in isopentane at -80°C . The embedded skins were sliced using a cryostat (CM3050; Leica Microsystems, Wetzlar, Germany) to obtain vertical 20 μm -thick sections. The prepared skin sections were observed with a confocal laser scanning microscope (CLSM; FV1000; Olympus Co., Tokyo, Japan).

Surface Distribution of Nanoparticles on Skin After commercial sunscreen containing titanium dioxide and zinc oxide nanoparticles had been applied to the excised porcine

ear skin (2 mg/cm²). TiO₂ and ZnO concentrations were 3.4% and 8.1%, respectively. The skin surface was observed using a scanning electron microscope (SEM, S-3400N; Hitachi High-Technologies Co., Tokyo, Japan). In addition, the skin distribution of carbon (C), titanium (Ti) and zinc (Zn) was observed using elemental mapping (EDX, X-Max50; Horiba Ltd., Kyoto, Japan). In this study, we used porcine ear skin, which is found to be similar barrier function to human skin¹⁴⁻¹⁶ and have larger the hair follicles than hairless rats.

RESULTS

In Vitro Skin Permeation of Fluoresbrite® Figure 1a shows the permeation profiles of Fluoresbrite® through needle-punctured skin. No permeation of Fluoresbrite® was observed not only through intact skin but also through stratum corneum-stripped skin over 24 h. In addition, interestingly, no permeation was found through the skin with deep razor wounds. On the other hand, Fluoresbrite® permeation into the receiver compartment was observed through needle-punctured skin treated by 20 to 30G needles (Fig. 1a). A decreased G number (*i.e.* increase in needle diameter) increased the skin permeation of Fluoresbrite® (Fig. 1a). The relation between Fluoresbrite® permeation and the external diameter and cross area of the needle was evaluated, and the results are shown in Figs. 1b and c, respectively. The result in Fig. 1b is a concave upward curve. The permeation of Fluoresbrite® through needle-punctured skin was almost proportional to the pore area

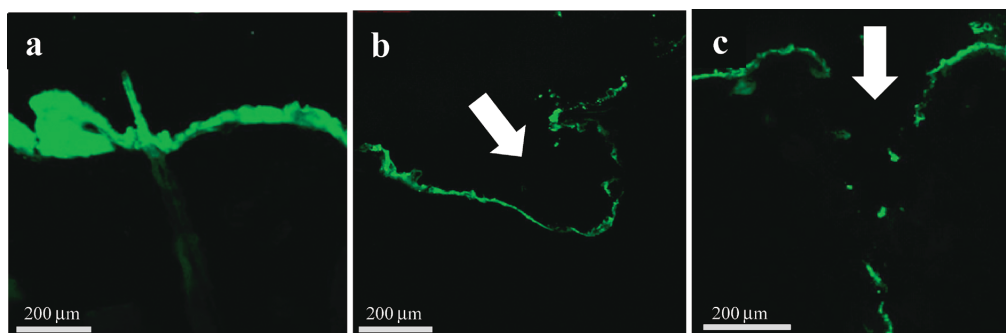
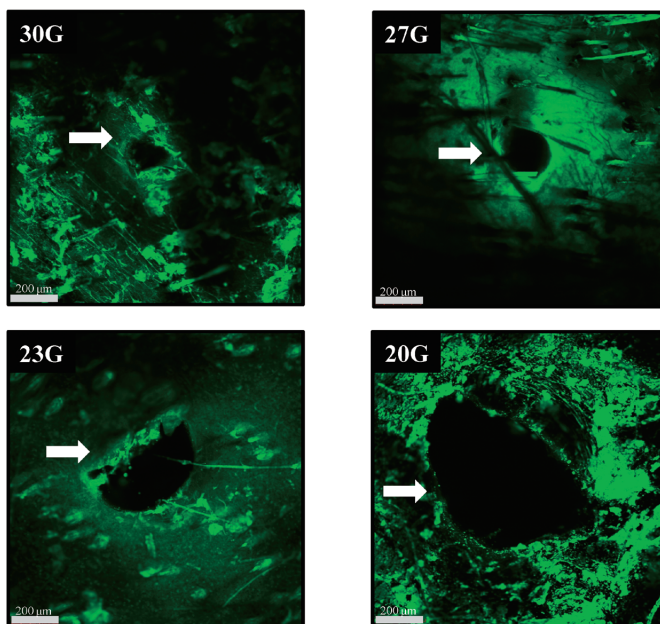


Fig. 2. CLSM Images of Vertical Slice of Hairless Rat Skin after Application of Fluoresbrite®

a: Stripped skin 24 h after application of Fluoresbrite®, b: razor-treated skin 5 min after application of Fluoresbrite®, and c: needle-punctured skin 10 min after application of Fluoresbrite®. Each bar represents 200 μ m. Arrows in b and c show sites of razor-treated and needle-punctured skin, respectively.

a) Epidermis side



b) Dermis side

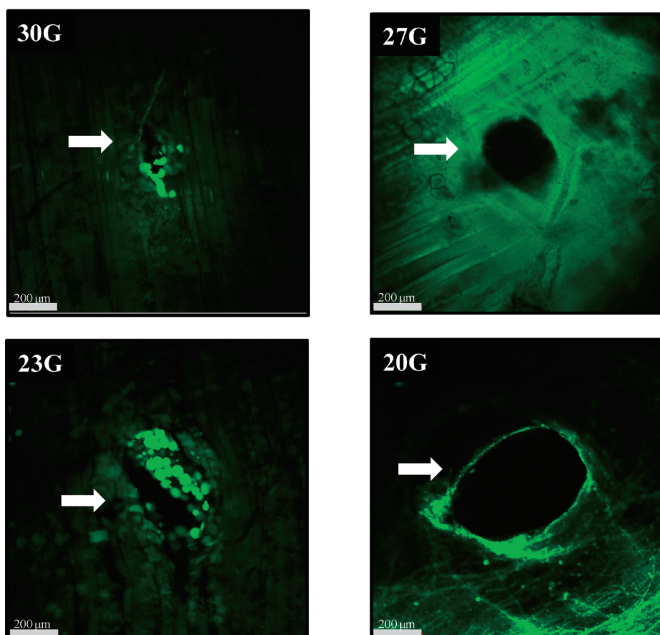


Fig. 3. CLSM Images of the Epidermis Side (a) and Dermis Side (b) of Needle-Punctured Hairless Rat Skin 5 min after Application of Fluoresbrite®

Arrows show pores created by needle puncture.

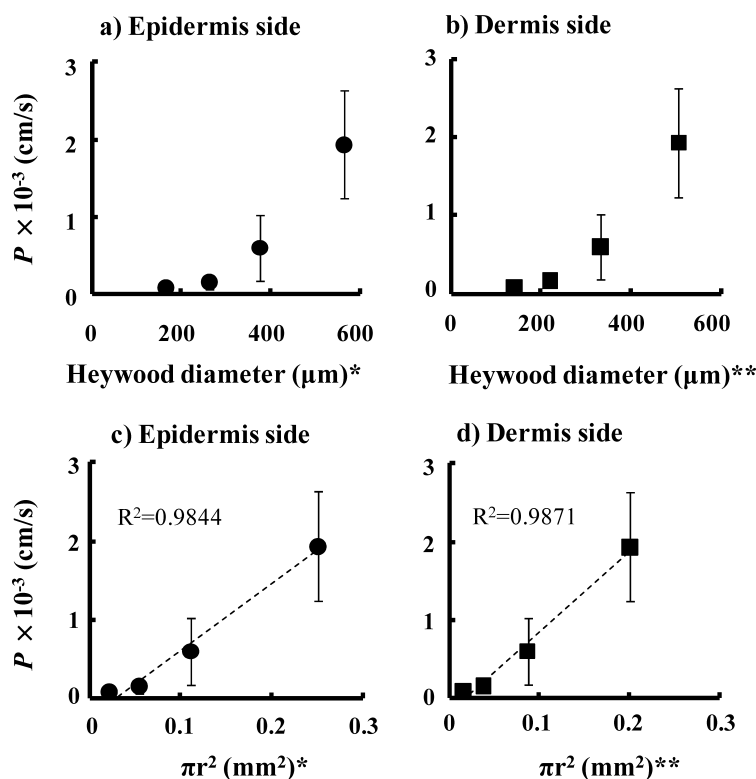


Fig. 4. Relationship between Permeability Coefficients (P) of Fluoresbrite® and Heywood Diameter (a,b) and Area (c,d) of Pores Prepared by Needle Puncture

Heywood diameter was calculated by CLSM observation from the epidermis side* and dermis side** of needle-punctured skin. The pore area was determined by $\pi \times (\text{Heywood diameter}/2)^2$. Intercepts in x-axis in Figs. 4c and d are 79 and 77 nm, respectively. The correlation coefficient was calculated by the liner regression. Each point represents the mean \pm S.E. ($n=3$).

made by the needle, as shown in Fig. 1c. The intercept of the abscissa axis was about 0.056 mm^2 .

Figure 2 shows CLSM images of a vertical slice of hairless rat skin after application of Fluoresbrite®. High fluorescence was found in the skin surface 24h after application to stripped skin (Fig. 2a). Detailed observation showed that the fluorescence was on the skin surface, not in the epidermis. Light fluorescence in the hair and around the hair follicles was probably related to autogenic fluorescence caused by hair protein. Since no fluorescence was found in the dermis, Fluoresbrite® did not permeate the viable epidermis and dermis. When Fluoresbrite® was applied to razor-treated skin, fluorescence was observed around the wound (Fig. 2b). When Fluoresbrite® was applied to needle-punctured skin, however, fluorescence was found across the pore made by the needle 10min after application (Fig. 2c). Fluoresbrite® could permeate skin very quickly *via* the perforating pathway. The width of the fluorescence in the deep skin site was much narrower than on the skin surface.

Figures 3a and b show CLSM images of the epidermis surface (a) and dermis surface (b) of needle-punctured excised hairless rat skin 5min after application of Fluoresbrite®. An increase in the external diameter of the needle from 30 to 20G increased the perforating pores made by the needles. Figures 4a and b show the effect of the Heywood diameter of the pores in the epidermal and dermal surfaces, respectively, made by needles on the permeability coefficient, P , of Fluoresbrite® through the skin. The P values increased with an increase in the Heywood diameter of the pores. These figures

(Figs. 4a,b) showed a concave upward curve, the same as in Fig. 1b. The relation between the P value and pore area was determined, and the results are shown in Figs. 4c and d. An almost straight line with an intercept of the abscissa axis was observed between the P value of Fluoresbrite® through the skin and pores made by needles, similar to Fig. 1c. The diameter was calculated to be about $80 \mu\text{m}$ from this intercept area. This size range may be needed for clear permeation of Fluoresbrite® of $0.05 \mu\text{m}$ (50 nm) in diameter through porous skin.

Figures 4a and b resemble Fig. 1b, and Figs. 4c and d also resemble Fig. 1c. Intercept of the abscissa axis in Fig. 1c was about 0.056 mm^2 , indicating $130 \mu\text{m}$ in diameter. The difference between 130 and $80 \mu\text{m}$ suggests shrinking of the pores in the skin after pulling out the needles.

Distribution of Nanoparticles on Skin after Application of Sunscreen Figures 5 and 6 show SEM photographs of the porcine skin surface after the application of commercial sunscreen cosmetics. Figure 5 compares a wide to narrow field of view of the skin surface. Each bar in Figs. 5a, b and c is 1.0mm, $200 \mu\text{m}$ and $50 \mu\text{m}$, respectively. White dots indicate sunscreen. Nanoparticles in sunscreen cosmetics were easily distributed in the groove, as shown in Fig. 5b, and hair follicles, as shown in Fig. 5c, after topical application.

Figure 6 shows SEM photographs and their elemental mapping on skin after the application of sunscreen cosmetics to porcine skin. Figures 6a–f show photographs of the same site containing hair follicles. Figure 6a is the original SEM photograph. Black areas in the figure are concentrated sunscreen. Figure 6b shows the distribution of carbon (C) on the skin in

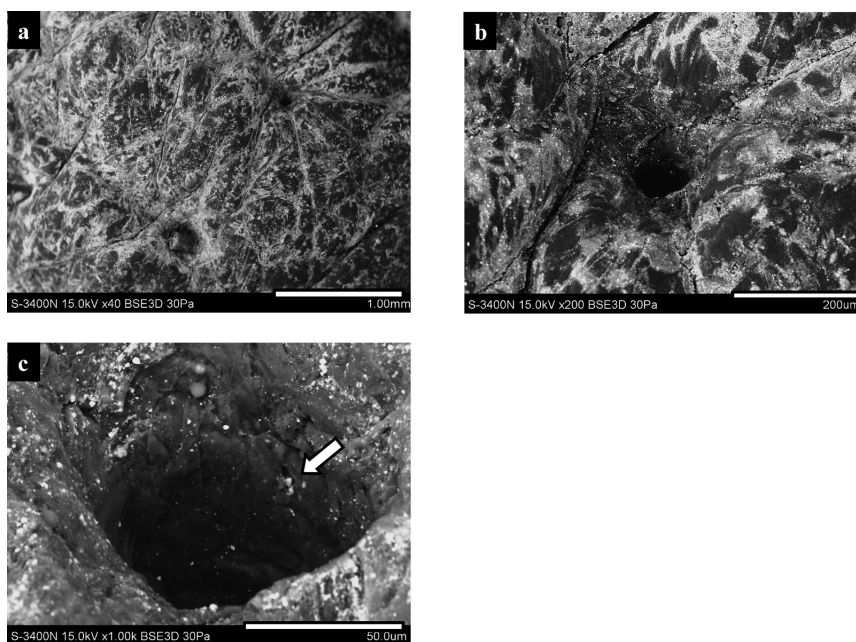


Fig. 5. SEM Images of Porcine Skin Surface after Application of Commercial Sunscreen

Arrow shows aggregated nanoparticles irrupting into hair follicles. Each white bar represents 1.0mm (a), 200 μ m (b), and 50 μ m (c).

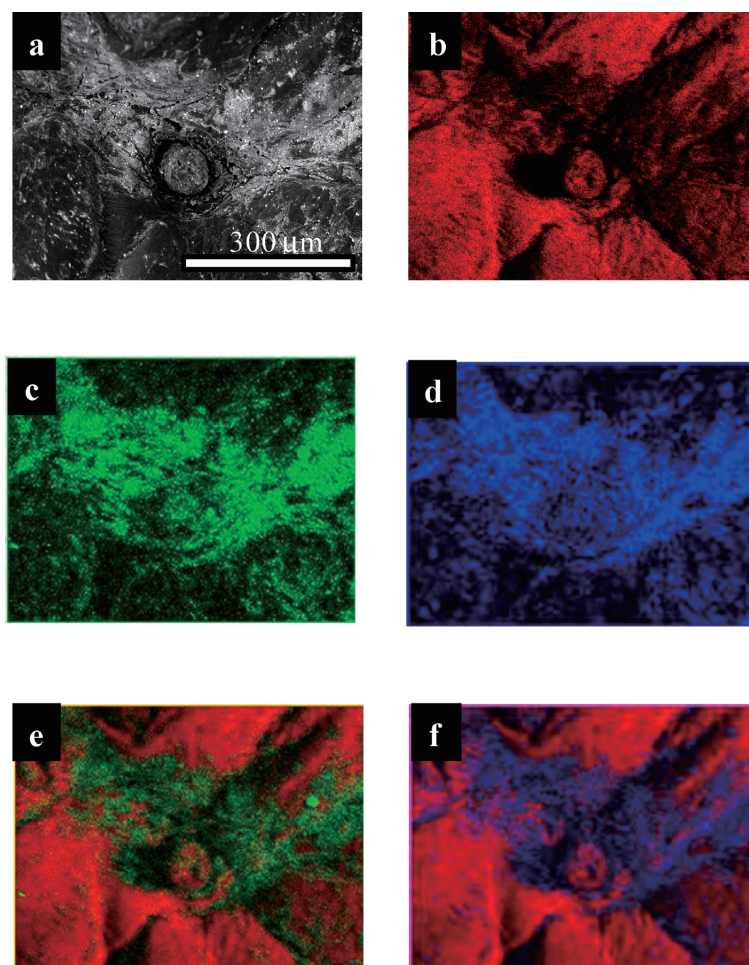


Fig. 6. SEM-EDX Elemental Mapping Images of Porcine Skin Surface after Application of Commercial Sunscreen

Original SEM image (a), carbon mapping (b), titanium mapping (c), zinc mapping (d), merged carbon and titanium mapping (e), and merged carbon and zinc mapping (f) of the same site of skin surface. A hair follicle was found almost center of the figure as clearly shown in Fig. 6a. Bar represents 300 μ m.

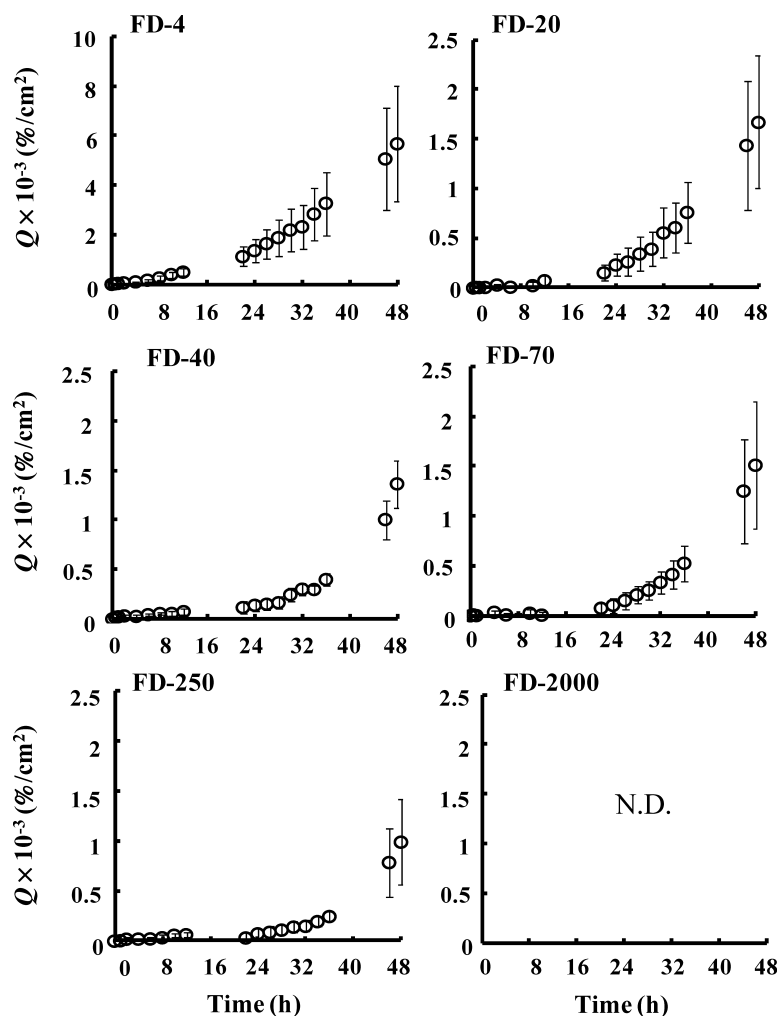


Fig. 7. Time Course of Changes in Cumulative Amount of FDs That Permeated Intact Hairless Rat Skin

Each point represents the mean \pm S.E. ($n=3-4$).

red, determined by elemental analysis. The red region is very similar to the black region in Fig. 6a, indicating low concentration of sunscreen. On the other hand, the distribution of Ti and Zn, as shown in Figs. 6c and d, respectively, is very similar, indicating a high concentration of sunscreen. In addition, these sites are very similar to the white region (high concentration of sunscreen) in Fig. 6a. Merged photographs of C+Ti and C+Zn, as shown in Figs. 6e and f, respectively, clearly suggest that titanium dioxide and zinc oxide nanoparticles are distributed in relatively deep regions, such as the groove and hair follicle infundibulum.

In Vitro Skin Permeation of FDs Skin permeation of model high molecular compounds, FDs, was also determined similarly to that of Fluoresbrite[®], and their permeability was compared. Figure 7 illustrates the time course of the cumulative amount of FD-4 to -2000 that permeated intact skin. FD-4 to -250 permeated intact skin, unlike the skin permeation of Fluoresbrite[®]. Intact skin permeability decreased with an increase in the molecular weight of FDs. A gradual increase over time was observed in the skin permeation of higher molecular weight FDs, which made it difficult to determine steady-state flux. FD-2000, with a solute diameter very similar to Fluoresbrite[®], did not permeate intact skin.

Figure 8 shows the permeation of FDs through stripped

skin or razor-treated skin. No change in the cumulative amount of FD-4 permeation over 8 h was observed through stripped skin and razor-treated skin, whereas higher permeation of FD-40 and FD-70 through razor-treated skin was observed than through stripped skin. The lack of difference in the permeation of FD-2000 through both types of skin may be due to low quantitative sensitivity.

Figure 9 shows a double logarithmic plot of the permeability coefficient, P , of FDs in cm/s, and the Stokes diameter, d , in nm of FDs. Log P of FDs through intact skin, stripped skin and razor-treated skin had a tendency to decrease with an increase in log d . The reason why log P of FD-70 was higher than FD-40, although there was not significant, is still unknown. Average P values for 22–36 h were used for intact skin, whereas steady-state P values were used for stripped-skin and razor-treated skin. The calculated maximum P value of FD-2000 was plotted for intact skin, since the receiver concentration was less than the quantification limit.

Figure 10 shows the effect of several treatments on the electric resistance of skin. The resistance of stripped skin was one twentieth that of intact skin. Similar data were observed for razor-treated skin. Interestingly, on the other hand, the electric resistance of needle-punctured skin was much higher than stripped skin and razor-treated skin. Fluoresbrite[®] only

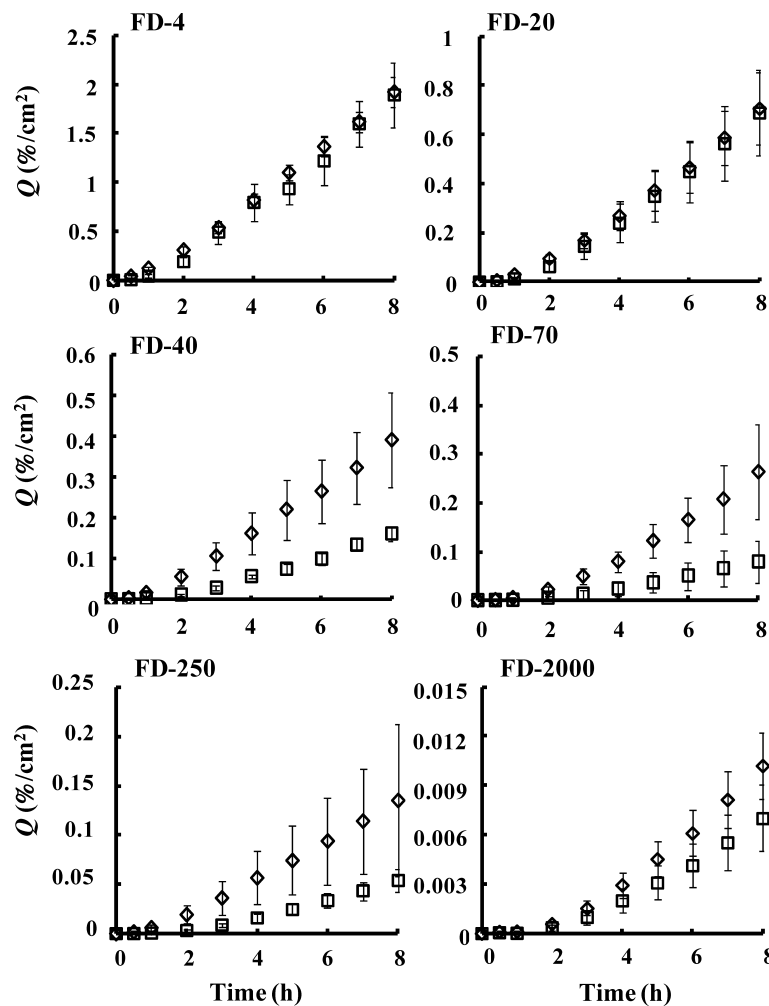


Fig. 8. Time Course of Changes in Cumulative Amount of FDs That Permeated Stripped and Razor-Treated Hairless Rat Skin
Each point represents the mean \pm S.E. ($n=3-4$).

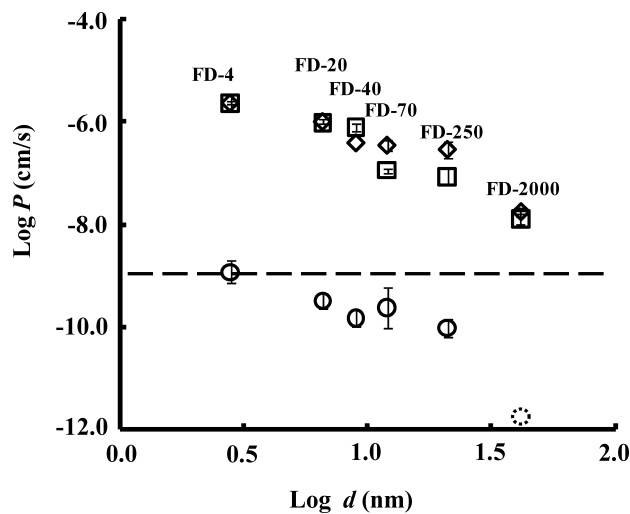


Fig. 9. Relationship between Permeability Coefficients (P) and Stokes Diameter (d) of FDs
Symbols: \circ : intact skin, \square : stripped skin, \diamond : razor-treated skin, \odot : FD-2000 estimated value. Dashed line shows desquamation rate. Each point represents the mean \pm S.E. ($n=3-4$).

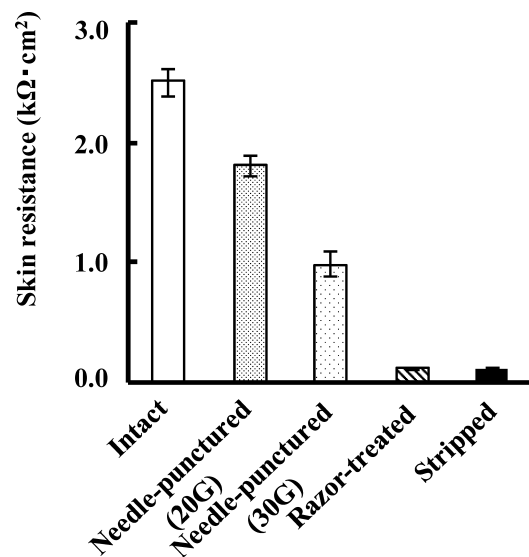


Fig. 10. Comparison of Electric Resistance in Several Hairless Rat Skin Samples 1h after Hydration
Each value represents the mean \pm S.E. ($n=4-5$).

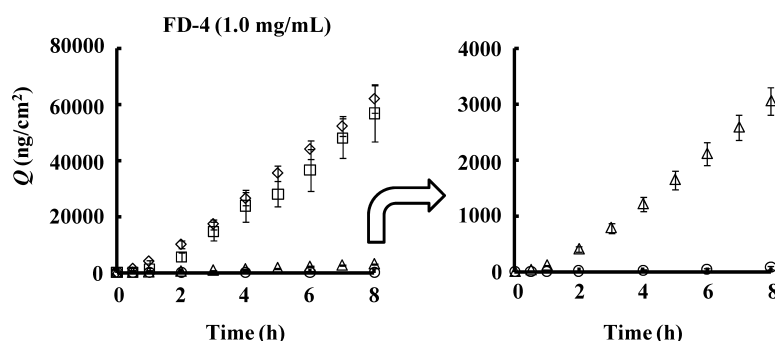


Fig. 11. Cumulative Amount in Several Skin Samples of FD-4

Symbols: ○: intact skin, □: stripped skin, ◇: razor-treated skin, △: needle-punctured skin. Each value represents the mean \pm S.E. ($n=3-4$).

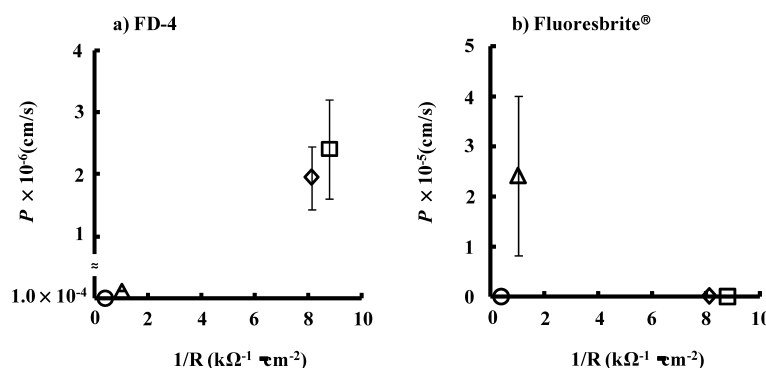


Fig. 12. Relationship between Permeability Coefficients (P) of FD-4 (a) or Fluoresbrite® (b) and Reciprocal of Electric Resistance in Several Skin Samples

Symbols: ○: intact skin, □: stripped skin, ◇: razor-treated skin, △: needle-punctured skin. Each value represents the mean \pm S.E. ($n=3-4$).

permeated needle-punctured skin, suggesting that its skin permeation was not reversely proportional to electric resistance.

Figure 11 shows the cumulative amount of FD-4 that permeated intact, stripped, razor-treated and needle-punctured skins. Unlike the skin permeation of Fluoresbrite®, FD permeation of skin increased with decreased skin resistance. Figure 12a shows the relation between the P value of FD-4 and the reciprocal of skin resistance. The figure shows that FD permeation of skin was almost proportional to the reciprocal of the electric resistance of skin. On the other hand, Fluoresbrite® permeation of skin was not dependent on skin resistance, as shown in Fig. 12b.

DISCUSSION

In Vitro Skin Permeation of Fluoresbrite® Since Fluoresbrite® did not permeate intact hairless rat skin, the P value of the nanomaterial through intact skin was calculated from the quantification lower limit. The calculated P value was less than 2.4×10^{-10} cm/s. This calculated P value is less than P_{des} , as shown in the theoretical section, and must be categorized as $P - P_{des} \ll 0$, suggesting that this type of nanomaterial does not permeate the greatest skin barrier, the stratum corneum. Furthermore, Fluoresbrite® did not permeate the viable epidermis and dermis, so-called stripped skin (Figs. 1a, 2a). Fluoresbrite® is not soluble in the majority of media; thus, it probably does not permeate a dissolution-diffusion membrane, a Type I membrane, explained in the theoretical section, although the nanomaterials may penetrate a cracked stratum

corneum, which may be a Type II membrane (porous membrane). A CLSM image of a vertical slice of hairless rat skin (Fig. 2a) showed that the fluorescence caused by Fluoresbrite® did not permeate stripped skin. In addition, fluorescence was observed on the wound surface after topical application to razor-treated skin (Fig. 2b). On the other hand, Fluoresbrite® could permeate the perforating pores made by needles (Figs. 1a, 2c). Fluoresbrite® permeation increased with an increase in the external diameter and cross sectional area of the needle (Figs. 1b,c) and the pore size (Fig. 4), indicating that the permeability of Fluoresbrite® was closely related to the pore area. CLSM images indicated that an increase in the external diameter of the needle from 30 to 20 G increased the pore area made by the needles (Fig. 3). It was suggested from the results in Fig. 4 that about 1000-fold greater pore size may be needed for sufficient penetration of Fluoresbrite® (50 nm in diameter). Thus, Fluoresbrite® did not permeate stripped skin or razor-treated skin, but permeated needle-punctured skin. The viable epidermis and dermis layer must be a significant barrier, as well as the stratum corneum, in the overall skin permeation of Fluoresbrite®. Zhang *et al.* reported that poly(D,L-lactic-co-glycolic acid) (PLGA) nanosphere did not permeate the holes-formed skin produced by micro-needles.¹⁷⁾ They concluded that these nanoparticles were distributed into the holes. Our results with their report suggest that insoluble nanoparticles may be permeated through big pores-existing skin membrane.

Distribution of Nanoparticles on Skin after Application of Sunscreen According to SEM images of the skin surface and elementary mapping, titanium dioxide and zinc oxide

nanoparticles tended to distribute around the groove and hair follicles after application of commercial sunscreen products (Figs. 5, 6). The results suggest that these nanoparticles must accumulate in the lower level of the average skin surface.¹⁸⁾ Recent papers^{19,20)} indicated that nanoparticles do not permeate skin; however, Jeong *et al.*,²¹⁾ Lademann *et al.*²²⁾ and Vogt *et al.*²³⁾ reported selective penetration of nanoparticles into hair follicles.^{21–24)} Our present data support these results.

In Vitro Skin Permeation of FDs FD-2000 with a similar solute diameter (41.6 nm) to Fluoresbrite® (50 nm) did not permeate intact skin (Fig. 7). This difference in the skin permeation of FD-2000 and Fluoresbrite® was probably due to different dissolution properties of these materials in application vehicles and skin: FD-2000 is soluble, but Fluoresbrite® is not. On the other hand, the permeability coefficient of FD-4 (solute diameter 3 nm) through intact skin was around 1×10^{-9} cm/s, similar to the desquamation rate of the upper corneocyte layer. As explained in the theoretical section, chemical materials with $P < 1 \times 10^{-9}$ cm/s did not permeate the stratum corneum under *in vivo* conditions; however, FD-4 permeated not only needle-punctured skin but also razor-treated and stripped skins (Figs. 7, 8). These results suggest that the primary barrier to the skin permeation of FD-4 is permeation of the stratum corneum. It was confirmed that the log *P* of FDs through the skin decreased with an increase in the logarithm of the molecular diameter of FD or log *d* (Fig. 9).

FD-4 was permeated through the intact skin as well as the damaged skin. The cumulative amount of FD-4 permeated through skin over 8 h was in an order of razor-treated > stripped > needle-punctured > intact skin (Fig. 11). The result was similar to the electric resistance, as illustrated in Fig. 10. Fluoresbrite® did not permeate stripped skin or razor-treated skin with low skin electric resistance, but penetrated needle-punctured skin with high skin resistance. In other words, the skin permeation of FDs well correlated with the reciprocal of skin resistance, whereas the skin permeation of Fluoresbrite® did not correlate with the reciprocal of skin resistance (Figs. 12a,b). Other FDs showed a similar tendencies as in FD-4. Therefore, soluble high molecular compounds slightly permeated skin, whereas insoluble nanoparticles did not permeate the viable epidermis or dermis. It is very important to be aware that insoluble nanoparticles may enter porous pathways, such as hair follicles and sweat glands.

CONCLUSION

Nanoparticles, which are considered not to dissolve in dispersion media or skin tissues, permeated only the porous pathway of skin to penetrate into the deep skin. Although they are distributed in the grooves and hair follicles, such insoluble nanoparticles can hardly diffuse in the viable epidermis and dermis. In conclusion, when considering the skin as a dissolution-diffusion membrane, nanoparticles (50 nm in average diameter) do not permeate or penetrate the skin; however, such nanoparticles may permeate a cracked stratum corneum and razor-treated skin. Thus, nanomaterials may affect viable cutaneous cells and, therefore, skin integrity is very important when nanomaterials are applied to the skin.

Acknowledgements This study was supported by a Grant-in-Aid for Scientific Research [H23-iyaku-sitei-016]

from the Ministry of Health, Labour, and Welfare, Japan.

REFERENCES

- 1) Hirose A, Nishimura T, Kanno J. Research strategy for evaluation methods of the manufactured nanomaterials in NIHS and importance of the chronic health effects studies. *Bull. Nat. Inst. Health Sci.*, **127**, 15–25 (2009).
- 2) German Chemical Industry Association. *Guidance for handling and use of nanomaterials at the workplace 2007*.
- 3) Steinberg DC. Regulations in chemicals, sunscreen labeling and nanotechnology. *Cosmetic and Toiletries Magazine*, **122**, 36–40 (2007).
- 4) Wu J, Liu W, Xue C, Zhou S, Lan F, Bi L, Xu H, Yang X, Zeng FD. Toxicity and penetration of TiO₂ nanoparticles in hairless mice and porcine skin after subchronic dermal exposure. *Toxicol. Lett.*, **191**, 1–8 (2009).
- 5) Schneider M, Stracke F, Hansen S, Schaefer UF. Nanoparticles and their interactions with the dermal barrier. *Dermatoendocrinology*, **1**, 197–206 (2009).
- 6) Schilling K, Bradford B, Castelli D, Dufour E, Nash JF, Pape W, Schulte S, Tooley I, van den Bosch J, Schellau F. Human safety review of “nano” titanium dioxide and zinc oxide. *Photochem. Photobiol. Sci.*, **9**, 495–509 (2010).
- 7) Filipe P, Silva JN, Silva R, Cirne de Castro JL, Marques Gomes M, Alves LC, Santos R, Pinheiro T. Stratum corneum is an effective barrier to TiO₂ and ZnO nanoparticle percutaneous absorption. *Skin Pharmacol. Physiol.*, **22**, 266–275 (2009).
- 8) Todo H, Kimura E, Yasuno H, Tokudome Y, Hashimoto F, Ikarashi Y, Sugibayashi K. Permeation pathway of macromolecules and nanospheres through skin. *Biol. Pharm. Bull.*, **33**, 1394–1399 (2010).
- 9) Alvarez-Román R, Naik A, Kalia YN, Guy RH, Fessi H. Skin penetration and distribution of polymeric nanoparticles. *J. Control. Release*, **99**, 53–62 (2004).
- 10) Sugibayashi K. Margin of safety and exposure of nanomaterials used in cosmetics. *Fragrance Journal*, **36**, 38–41 (2008).
- 11) Sigma-Aldrich, Co., *Certificate of analysis*.
- 12) Jyoti KJ, Sabyasachi C, Norma WA, Sanford MS. Synaptotagmin VII Restricts Fusion Pore Expansion during Lysosomal Exocytosis. *PLoS Biol.*, **2**, 1225–1232 (2004).
- 13) Kraneveld AD, Koster AS, Nijkamp FP. Microvascular permeability in isolated vascularly perfused small intestine of rats. *Am. J. Physiol.*, **266**, G1170–G1178 (1994).
- 14) Wu X, Price GJ, Guy RH. Disposition of nanoparticles and an associated lipophilic permeant following topical application to the skin. *Mol. Pharm.*, **6**, 1441–1448 (2009).
- 15) Sekkat N, Kalia YN, Guy RH. Biophysical study of porcine ear skin *in vitro* and its comparison to human skin *in vivo*. *J. Pharm. Sci.*, **91**, 2367–2381 (2002).
- 16) Simon GA, Maibach HI. The pig as an experimental animal model of percutaneous permeation in man: qualitative and quantitative observations—An overview. *Skin Pharmacol. Appl. Skin Physiol.*, **13**, 229–234 (2000).
- 17) Zhang W, Gao J, Zhu Q, Zhang M, Ding X, Wang X, Hou X, Fan W, Ding B, Wu X, Wang X, Gao S. Penetration and distribution of PLGA nanoparticles in the human skin treated with microneedles. *Int. J. Pharm.*, **402**, 205–212 (2010).
- 18) Allec J, Chatelus A, Wagner N. Skin distribution and pharmaceutical aspects of adapalene gel. *J. Am. Acad. Dermatol.*, **36**, S119–S125 (1997).
- 19) Gamer AO, Leibold E, van Ravenzwaay B. The *in vitro* absorption of microfine zinc oxide and titanium dioxide through porcine skin. *Toxicol. In Vitro*, **20**, 301–307 (2006).
- 20) Senzui M, Tamura T, Miura K, Ikarashi Y, Watanabe Y, Fujii M. Study on penetration of titanium dioxide (TiO₂) nanoparticles into intact and damaged skin *in vitro*. *J. Toxicol. Sci.*, **35**, 107–113

- (2010).
- 21) Jeong SH, Kim JH, Yi SM, Lee JP, Kim JH, Sohn KH, Park KL, Kim MK, Son SW. Assessment of penetration of quantum dots through *in vitro* and *in vivo* human skin using the human skin equivalent model and the tape stripping method. *Biochem. Biophys. Res. Commun.*, **394**, 612–615 (2010).
- 22) Lademann J, Richter H, Teichmann A, Otberg N, Blume-Peytavi U, Luengo J, Weiss B, Schaefer UF, Lehr CM, Wepf R, Sterry W. Nanoparticles—An efficient carrier for drug delivery into the hair follicles. *Eur. J. Pharm. Biopharm.*, **66**, 159–164 (2007).
- 23) Vogt A, Combadiere B, Hadam S, Stieler KM, Lademann J, Schaefer H, Autran B, Sterry W, Blume-Peytavi U. 40 nm, but not 750 or 1500 nm, nanoparticles enter epidermal CD1a+ cells after transcutaneous application on human skin. *J. Invest. Dermatol.*, **126**, 1316–1322 (2006).
- 24) Toll R, Jacobi U, Richter H, Lademann J, Schaefer H, Blume-Peytavi U. Penetration profile of microspheres in follicular targeting of terminal hair follicles. *J. Invest. Dermatol.*, **123**, 168–176 (2004).